ISSN: 1803-3814

MENDEL Soft Computing

A NUMERICAL CHARACTERIZATION OF NANOPARTICLE DISTRIBUTION ON SURFACE OF A SEMICONDUCTOR

Zdena Rudolfová, Jana Hoderová

University of Technology
Institute of Physical Engineering, FME
Technická 2, 616 69 Brno
Czech Republic
zdenadr@seznam.cz

University of Technology
Institute of Mathematics, FME
Technická 2, 616 69 Brno
Czech Republic
hoderova@fme.vutbr.cz

Abstract: *The motivation for this work was to qualitatively describe the distribution of Au nanoparticles on the surface of a semiconductor. We discuss suitable mathematical characteristics which allow the uniform distribution to be distinguished from the distribution affected by any physical phenomenon, i.e. by the repulsive force between electrically charged particles or by the influence of properties of the surface. We identify Voronoi decomposition and a statistical analysis of Voronoi cell properties as a suitable tool for this purpose.*

Keywords: *distribution, Voronoi diagram, hypothesis testing, Legendre ellipse, 4PL function, nanoparticles*

1 Introduction

Let us consider an image created by electron microscope of the specimen whose surface is more or less covered by nanoparticles. For the detection of particles in the image, a threshold method is used [2]. After the detection, the particles which touch each other are separated using the method developed by Pavel Šťarha [3, 4]. The method is based on the geometric properties of the object of interest and on the assumptions made regarding the shape of the elementary objects. Then, the centroid is computed for every particle and the Voronoi decomposition is done.

2 Voronoi decomposition and moment characteristics

A Voronoi diagram is a partitioning of a plane into regions based on distance to points in a specific subset of the plane. In our case the set of points (called generators) are centroids of nanoparticles. For each generator there is a corresponding region (called Voronoi cell) consisting of all points closer to that generator than to any other. All the image of surface with nanoparticles is decomposed into Voronoi cells, see Fig. 1. Then the size of areas of these Voronoi cells can be statistically analyzed to determine whether the nanoparticles on the surface are distributed with 2D uniform distribution or exhibit a statistically significant deviation from this distribution.

The size of areas of the Voronoi cells will be our field of interest for following statistical analysis based on the moment characteristics up to third order. Let us denote $p'(D_i)$ the size of area of Voronoi cell D_i in pixels. Normalized size of area of D_i is defined as

$$p(D_i) = \frac{p'(D_i)}{\frac{1}{n}\sum_{j=1}^{n} p'(D_j)} \tag{1}$$

where n is number of particles in the image. Standard deviation σ and skewness ψ of the normalized size of area is

$$\sigma = \sqrt{\frac{1}{n-1}\sum_{i=1}^{n}\left(p(D_i)-1\right)^2}, \qquad \psi = \frac{1}{\sigma^3 n}\sum_{i=1}^{n}\left(p(D_i)-1\right)^3. \tag{2}$$

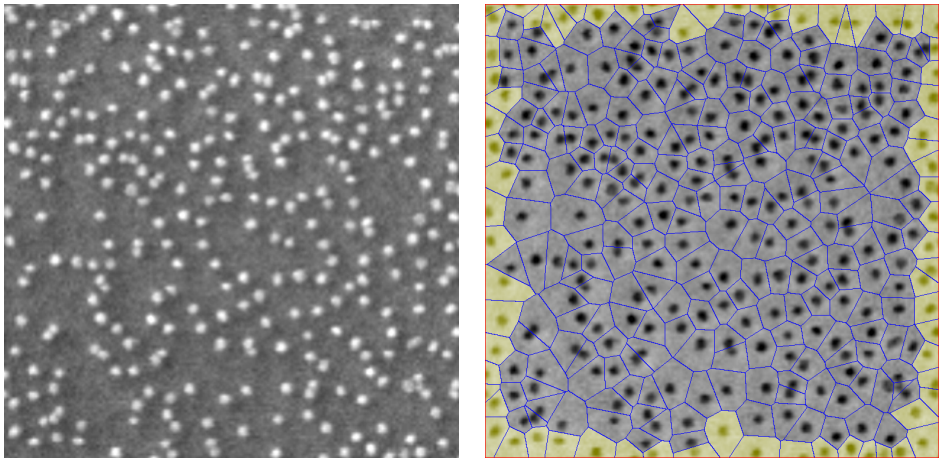

Figure 1: Real-image of the semiconductor GaAs which was immersed in a solution of amino acid Lysine for 30 s and in a solution of 20 nm Au nanoparticles for 10 min created by electron microscope (on the left) and its Voronoi decomposition (on the right). The real size of the image is 1×1 μm.

3 Properties of the Voronoi decomposition for uniform distribution

Since there is no available theory for analyzing moment characteristics for 2D uniform distribution of generators of Voronoi decomposition, we will solve this problem by computer simulation. For this, the Borland Delphi was used. In a uniform distribution, 125, 250, 500, 1000, 2000 and 4000 particles were placed randomly into the image. For each number set, 10000 simulations of Voronoi decomposition were carried out and, for each simulation, moment characteristics were computed. From this data, point estimations of the standard deviation σ and the skewness ψ were computed (see Table 1).

Table 1: Point estimations of the parameters σ, ψ

n	σ	ψ
125	0.5262	0.8830
250	0.5294	0.9572
500	0.5311	0.9933
1000	0.5318	1.0121
2000	0.5321	1.0126
4000	0.5331	1.0043

The main problem with formulation of the hypothesis that particles are uniformly distributed based on knowledge of σ and ψ for the experimental images, is that we must consider 2 quantities at the same time. We have to consider vector (σ, ψ) whose components are not independent (both of them are computed by arithmetic mean) and, also, it is known that for random vector there is no analogical theory of the interval estimation of one observed value (because in $\mathbb{R}^2$ ordering doesn't exist).

We would like to find out a method for testing statistical hypothesis of particles on the surface which have uniform distribution.

4 Histograms of experimental data and their representation

For the next analysis of properties of Voronoi decomposition obtained by the set of generators with 2D uniform distribution of the particles, the histograms of vector (σ,ψ) are created for number of particles $n = 125, 250, 500, 1000, 2000, 4000$. Those histograms are represented as digital images, where coordinates of the pixels in the image are given by bins of vector (σ, ψ) and frequency of each bin is represented by the pixel value, see Fig. 2. The number of simulations is 10000. Very important is the choice of number of bins in the histogram. The aim is to obtain 400 (the number was chosen on the basis of simulations) non-empty bins of histogram so that we get continuous sets of pixels by the threshold method applied on the histogram. The shape of the histograms in images in Fig. 2 is similar to that of an ellipse. Therefore, the ellipse (in our case it is a Legendre ellipse [1]) was chosen for the approximation of the set (this set we denote G) to which the vector (σ, ψ) belongs with specified probability τ. If we find the parameters of the ellipse, we can test that the distribution of particles is uniform on the $(1 - \tau)$ level of significance.

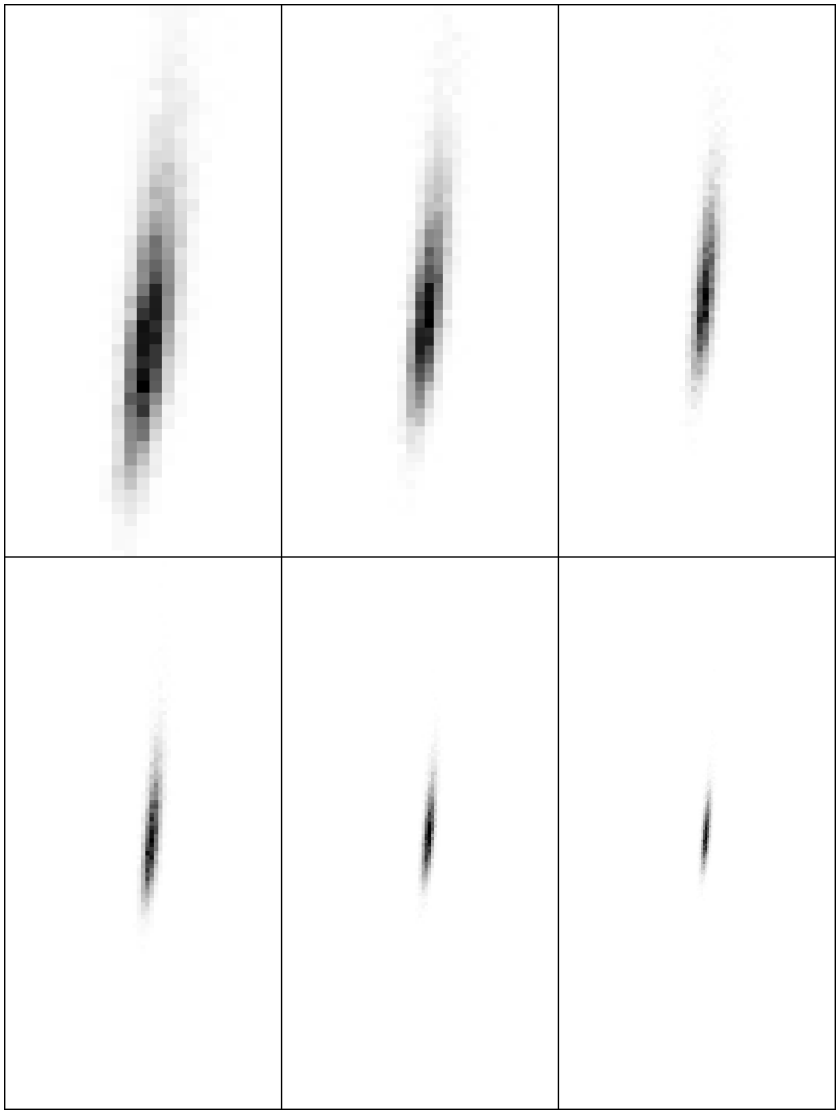

Figure 2: Histograms H_{125}, H_{250}, H_{500} (in the upper part) and histograms H_{1000}, H_{2000}, H_{4000} (in the lower part). Size of each rectangle represents interval $\sigma \in \langle 0, 1\rangle$ in horizontal direction and $\psi \in \langle 0, 2\rangle$ in vertical direction. Histogram negatives are shown for clarity, i.e. empty bin of the histogram has white color and the bin of maximum frequencies is black. For better visualization on the paper, the pictures were cropped but for mathematical analysis we used vertical range $\psi \in \langle 0, 4\rangle$. The optimization of the number of histogram bins is clear from the images. Although histograms have a significantly different number of bins, the number of non-empty bins is the same (400).

The Legendre ellipse is an ellipse with the center in the centroid and with the same geometrical moments up to the second order as the original area G. Definition of the geometric moments of the object G is

$$m_{i,j}(G) = \iint_G \sigma^i \psi^j \, \mathrm{d}\sigma \, \mathrm{d}\psi, \tag{3}$$

where $i, j = 0, 1, 2, \ldots$ and $i + j$ denotes order of the moment. Then, the center of ellipse $S = [\sigma_S, \psi_S]$ in the Cartesian coordinate system $\sigma\psi$ is computed as

$$S = \left[\frac{m_{1,0}(G)}{m_{0,0}(G)}, \frac{m_{0,1}(G)}{m_{0,0}(G)}\right]. \tag{4}$$

Orientation of major and minor axis of the ellipse is derived from central moments [1]

$$\overline{m}_{i,j}(G) = \iint_G (\sigma - \sigma_S)^i (\psi - \psi_S)^j \, \mathrm{d}\sigma \, \mathrm{d}\psi \tag{5}$$

and the directions of semi-axes of the ellipse are given by angles

$$\varphi_k = \frac{1}{2}\text{arctg}\frac{2\overline{m}_{1,1}(G)}{\overline{m}_{2,0}(G) - \overline{m}_{0,2}(G)} + \frac{k\pi}{2}, \quad k = 0, 1, 2, 3. \tag{6}$$

We will continue in the text with the simplified notation of the angle φ for the major axis. If we declare a coordinate system $\sigma\psi$ as the basic coordinate system, the new coordinate system $\sigma'\psi'$ with the origin in S and axis σ' in the direction of major axis of ellipse and ψ' given by direction of the minor axis of the ellipse we will denote as the principal coordinate system $\sigma'\psi'$. Let us denote central moments of the object G in the principal coordinate system $\sigma'\psi'$ by $m^{\star}_{i,j}(G)$. Then, for the semi-major axis a and for the semi-minor axis b it holds that

$$a = 2\sqrt{m^{\star}_{2,0}(G)}, \quad b = 2\sqrt{m^{\star}_{0,2}(G)} \tag{7}$$

and for elongation ε of the Legendre ellipse of the object G it holds that

$$\varepsilon = \log_2 \frac{a}{b}. \tag{8}$$

You can see parameters of the Legendre ellipse obtained from 10000 simulations in Table 2 (processing was done using the software SOFO ACC 6.0.) and the sample case of Legendre ellipse in Fig. 3.

Table 2: Parameters of the Legendre ellipse derived from images of the histograms H_{125}, $H_{250}, \ldots H_{4000}$.

n	$\ln n$	σ_S	ψ_S	φ	ε
125	4.82831	0.52594	0.87935	84.28°	2.809
250	5.52146	0.52926	0.95501	84.74°	2.978
500	6.21640	0.53101	0.99123	85.00°	3.147
1000	6.90775	0.53168	1.01056	85.22°	3.241
2000	7.60090	0.53176	1.01041	85.73°	3.259
4000	8.29404	0.53268	1.00191	85.81°	3.265

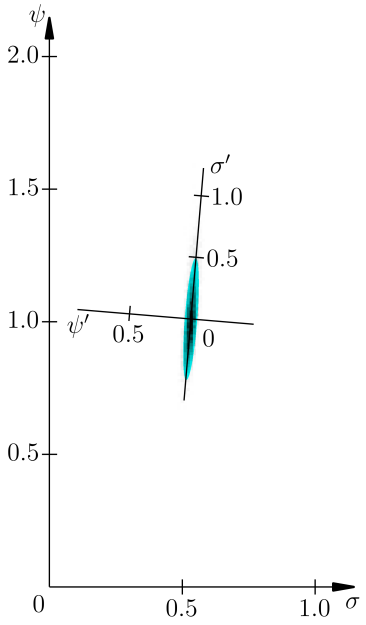

Figure 3: The Legendre ellipse derived from the image of the histogram H_{1000} for probability $\tau = 0.99$ (see Section 5). In the picture there is drawn a basic coordinate system $\sigma\psi$ and also the principal coordinate system $\sigma'\psi'$.

5 Optimization of the parameters of the Legendre ellipse

We know the center S, elongation ε and orientation of the Legendre ellipse given by angle φ at the moment. The length of the semi-major axis a and semi-minor axis b can be computed so that for a given number of particles n

is the probability that the parameters σ and ψ of the Voronoi decomposition for the uniform distribution of particles belong into ellipse is equal to the specified probability τ.

Let us denote $L(a, b)$ Legendre ellipse with the length of semi-major axis a and semi-minor axis b and let us denote $q = \tau m$, where $m = 10000$ is the number of simulations. We define the set

$$Q(a, b) = \{i \in \{1, 2, \dots m\} \mid [\sigma_i, \psi_i] \in L(a, b)\}, \tag{9}$$

where $[\sigma_i, \psi_i]$ are the values obtained by ith simulation. Let us denote $|Q(a, b)|$ the number of elements of this set (it is the number of elements which belong into Legendre ellipse $L(a, b)$ within m simulations). The lengths a and b were computed iteratively in the sense of the bisection method. The idea of this process is that we choose initial lower and upper estimates for the lengths a and b (notation for ith estimations are $a_{d,i}$, $a_{h,i}$, $b_{d,i}$ and $b_{h,i}$) and initial estimates of $|Q(a_{d,1}, b_{d,1})|$ and $|Q(a_{h,1}, b_{h,1})|$. By the bisection method we compute

$$a_{d,i+1} = \begin{cases} a_{d,i} & \text{pro} \quad |Q(a_{c,i}, b_{c,i})| > q \\ a_{c,i} & \text{pro} \quad |Q(a_{c,i}, b_{c,i})| \leq q \end{cases}, \quad a_{h,i+1} = \begin{cases} a_{h,i} & \text{pro} \quad |Q(a_{c,i}, b_{c,i})| \leq q \\ a_{c,i} & \text{pro} \quad |Q(a_{c,i}, b_{c,i})| > q, \end{cases} \tag{10}$$

where

$$a_{c,i} = \frac{a_{d,i} + a_{h,i}}{2} \tag{11}$$

and our stop criterium is

$$|Q(a_{c,i+1}, b_{c,i+1})| = |Q(a_{c,i}, b_{c,i})|, \tag{12}$$

i.e. we will stop the iteration if the change in the lengths a and b does not lead to a more accurate result.
In order to determine whether $[\sigma_i, \psi_i]$ belongs $L(a, b)$, we come out of the focal features of the ellipse.
In this way, the a and b values were obtained depending on the number of particles n in the image and the specified probabilities τ. Three probabilities were chosen $\tau = 0.90,\ 0.95,\ 0.99$. An overview of the results is found in Table 3.

Table 3: Lengths of the Legendre ellipse semi-axes a, b depending on the number of particles n in the image and probability τ.

τ	n	$\ln n$	a	b
0.90	125	4.82831	0.71289	0.101688
0.90	250	5.52146	0.55664	0.070748
0.90	500	6.21460	0.41992	0.047234
0.90	1000	6.90775	0.32226	0.034266
0.90	2000	7.60090	0.22460	0.023449
0.90	4000	8.29404	0.16601	0.017232
0.95	125	4.82831	0.83007	0.118404
0.95	250	5.52146	0.65429	0.083160
0.95	500	6.21460	0.47851	0.053825
0.95	1000	6.90775	0.36132	0.038420
0.95	2000	7.60090	0.26367	0.027527
0.95	4000	8.29404	0.18554	0.019260
0.99	125	4.82831	1.20117	0.171337
0.99	250	5.52146	0.96679	0.122878
0.99	500	6.21460	0.69335	0.077992
0.99	1000	6.90775	0.49804	0.052957
0.99	2000	7.60090	0.34179	0.035684
0.99	4000	8.29404	0.22460	0.023315

6 Calculation of the parameters of the Legendre ellipse for general number of particles

The next step in the generalizing method for determining the parameters of the Legendre ellipse is to find an algorithm for the general number of particles. We use four parameter logistics function Λ (4PL function) for the approximation of all parameters of the Legendre ellipse in the form

$$\Lambda(x) = D + \frac{A - D}{1 + \left(\frac{x}{C}\right)^B}, \tag{13}$$

where $x = \ln n$ and n is the number of the particles into the image. Based on the parameters in Table 2, approximations were computed using 4PL functions. The result is the coefficients A, B, C, D of the 4PL functions, which are listed in Table 4 and the graphs corresponding to the approximating 4PL functions are shown in Fig. 4 and 5.

Table 4: Parameters of the 4PL function $\Lambda(x)$, $x = \ln n$ for approximation of parameters of the Legendre ellipse.

	A	B	C	D
σ_S	-381.0125	3.774573	0.2760439	0.5339951
ψ_S	0.8391545	13.76506	5.217051	1.010437
φ	43.10296	0.09565836	100239.3	170.9187
ε	2.738589	12.32581	5.621842	3.272467

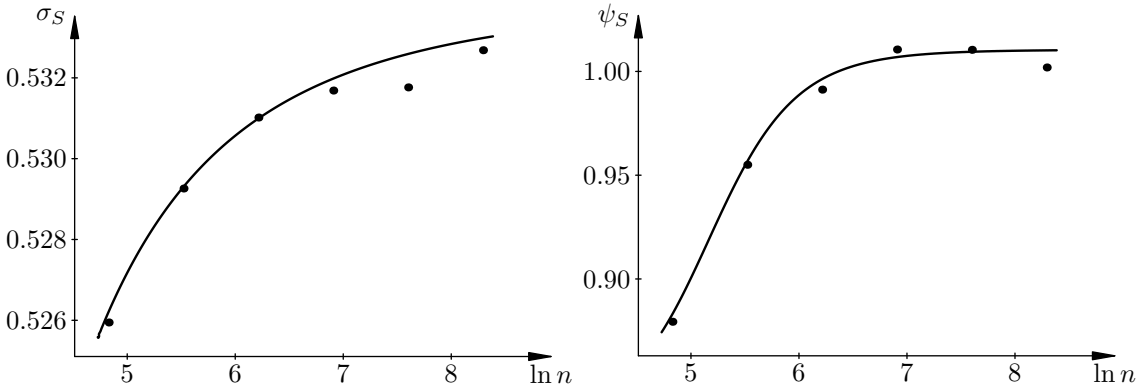

Figure 4: The graphs of the 4PL functions $\Lambda(x)$, $x = \ln n$ for the coordinates of the center of the Legendre ellipse $S[\sigma_S, \psi_S]$.

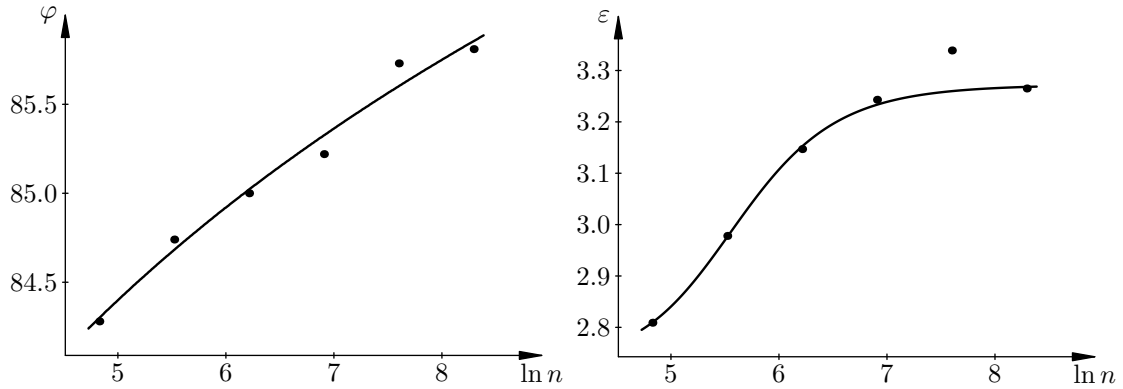

Figure 5: The graphs of the 4PL functions $\Lambda(x)$, $x = \ln n$ for the major axes slope described by the angle φ and elongation ε.

We computed the 4PL functions $\Lambda(x)$, $x = \ln n$ for an approximation of the lengths of major-axes a and minor-axes b using parameters in Table 3, for probabilities $\tau = 0.90,\ 0.95,\ 0.99$. The graphs of these functions are in Fig. 6.

7 Testing of hypothesis that the distribution of the particles in the image is uniform.

We will test the hypothesis that real-image of particle distribution has a 2D uniform distribution, i.e. that it is not possible to statistically demonstrate the influence of mutual relationship between particles or surface effect on particle distribution. We select the level of significance $(1 - \tau)$ (probability that the hypothesis holds and we will reject it) and construct the Legendre ellipse L for probability τ. We calculate the parameters σ and ψ for

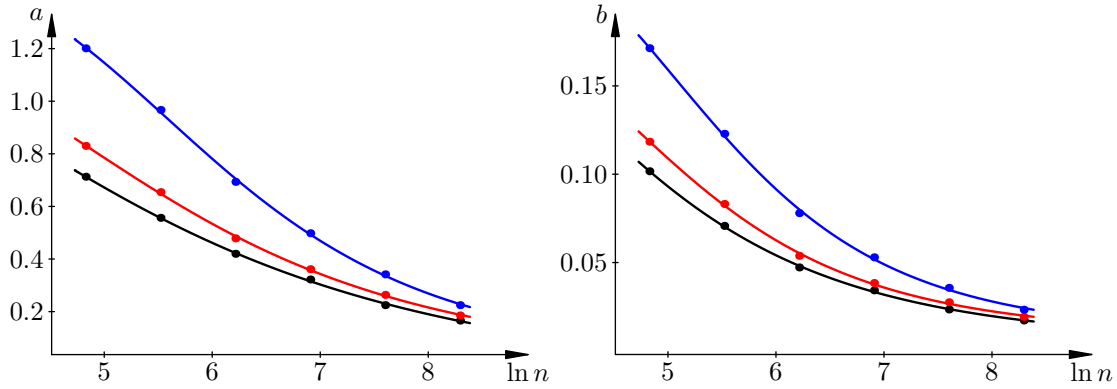

Figure 6: The graphs of the 4PL functions $\Lambda(x)$, $x = \ln n$ for the length of semi-major axes a and semi-minor axes b. For $\tau = 0.90$ by the solid lines, for $\tau = 0.95$ by the dashed lines and for $\tau = 0.99$ by the dotted line.

the Voronoi decomposition of the test image. We accept the hypothesis in the case $[\sigma, \psi] \in L$. All other cases, we will reject it. There is graphical representation of the test of the hypothesis on $(1 - 0.95)$ level of significance in Fig. 7. The hypothesis is rejected in this case because $[\sigma, \psi]$ doesn't belong to the Legendre ellipse.

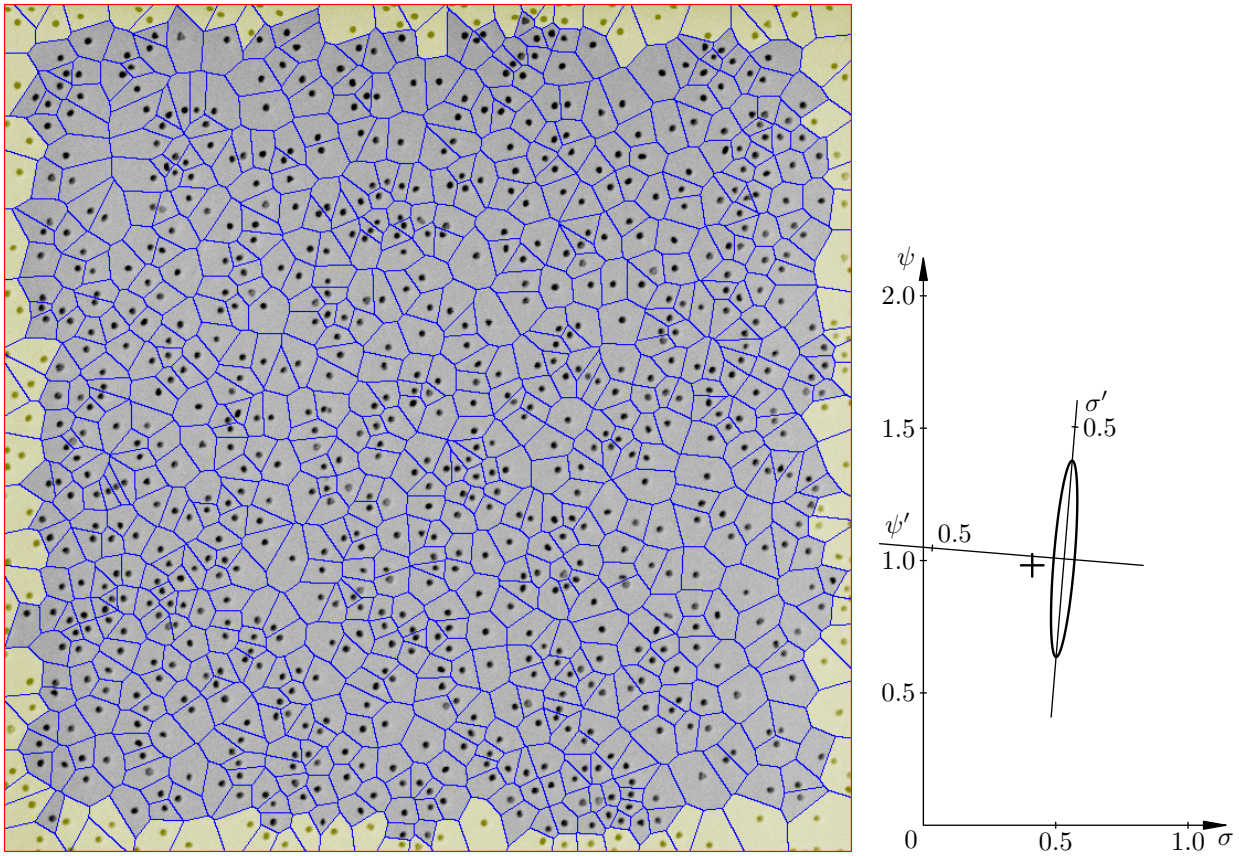

Figure 7: Voronoi decomposition of the real-image with $n = 920$ nanoparticles created by electron microscope (on the left) and corresponding Legendre ellipse with the result of the test of the hypothesis on 0.05 level of significance. The cross (i.e. position of parameters $[\sigma, \psi]$) outside the ellipse determine that the hypothesis was rejected.

8 Conclusion

This paper is solving nontrivial problem of testing hypothesis of the random vector which has dependent components. There is no general solution of this problem and no general theory exists. Therefore, this unique method has been developed. Benefit of this method is that it enables to distinguish the detection of structural changes which are not possible to find without described algorithm. The principal presented in this paper is

general and it is possible to apply in any test of particle distribution in the case that it is possible to simulate the theoretical distribution of particles.

Acknowledgement: This work is an output of research and scientific activities of NETME Centre, regional R&D centre built with the financial support from the Operational Programme Research and Development for Innovations within the project NETME Centre (New Technologies for Mechanical Engineering), Reg. No. CZ.1.05/2.1.00/01.0002 and, in the follow-up sustainability stage, supported through NETME CENTRE PLUS (LO1202) by financial means from the Ministry of Education, Youth and Sports under the "National Sustainability Programme I".

References

[1] Flusser, J., Suk, T., Zitová, B.: Moments and Moment Invariants in Pattern Recognition, Wiley & Sons Ltd., 312 pp. (2009)

[2] Pratt, W. K.: Digital image processing: PIKS Scientific inside. 4th ed., Newly updated and rev. ed. Hoboken, N.J.: Wiley-Interscience (2007)

[3] Štarha, P., Druckmüllerová, H.: Decomposition of a Bunch of Objects in Digital Image. In: *Combinatorial image analysis: 16th International Workshop, IWCIA, Brno, Czech Republic, May 28-30, 2014. Proceedings*. 1st edition. Berlin: Springer International Publishing (2014)

[4] Štarha, P., Martišek, D., Matoušek, R.: Numerical Method of Object Reconstruction Using Moment Method. In: Mendel 2014: 20 th international conference on soft computing: evolutionary computation, genetic programming, fuzzy logic, rough sets, neural networks, fractals, bayesian methods: June 15-17, 2011, Brno, Czech Republic. Brno: University of Technology (2014)